Target Tracking for Wireless Localization Systems Using Set-Membership Filtering: A Component-Based Event-Triggered Mechanism ⋆

Xingzhen Bai [a], Zidong Wang [a,b,∗], Lei Zou [b], Zhijing Zhang [a]

[a] *College of Electrical Engineering and Automation, Shandong University of Science and Technology, Qingdao 266590, China*

[b] *Department of Computer Science, Brunel University London, Uxbridge, Middlesex, UB8 3PH, United Kingdom*

Abstract

This paper is concerned with the target tracking problem for a class of wireless localization systems with unknown but bounded noises. Since the energy supply of wireless sensor nodes is rather scarce, a component-based event-triggered mechanism is utilized to reduce the signal transmission frequency by discarding the unnecessary information transmissions. The objective of the addressed problem is to design an event-triggered set-membership filter for target tracking with guaranteed performance. An estimate-based linearization approach is employed to reconstruct the innovation and a particle swarm optimization (PSO) algorithm is adopted to determine the uncertain scaling matrix generated by the linearization. The desired time-varying filter gain matrix is derived by solving a convex optimization problem. Finally, the personnel safety monitoring problem in a mine industrial site is considered in the simulation experiment to demonstrate the effectiveness of the proposed filtering algorithm.

Key words: Target tracking, wireless localization system, set-membership filtering, event-triggered mechanism, energy conservation.

1 Introduction

With the rapid development of the modern industry, the safety problem has become a primary concern in the industrial manufacturing process. Since the unpredictable accidents are likely to cause unexpected losses and casualties, it is highly urgent to develop effective personnel/equipment monitoring systems in industrial sites. In particular, the wireless localization system plays a key role in the personnel monitoring to guarantee the safety of personnel working under hazardous environmental conditions. The wireless localization systems generally utilize advanced informative facilities of wireless transmission networks, where the wireless intelligent nodes are capable of sensing data locally and collaborating with other sensor nodes to exchange relevant information about the monitored objects [26]. In practical engineering, the wireless localization systems have been widely applied in industrial sites to track the personnel and mobile equipment [7], which are able to enhance the perception capability of security information in the industrial monitoring system.

It is quite common in industrial sites that the wireless communication environment is complex, and various kinds of measurement noises and interferences are inherent to the environment [24]. Furthermore, the distance between the sensor nodes and the target of interest is often modeled by certain nonlinear functions, which gives rise to the nonlinear filtering problem. As such, various nonlinear filters (e.g. extended Kalman filter (EKF), unscented Kalman filter (UKF) and particle filter (PF)) have been developed in the past decades. Specifically, the EKF is based on the first-order linearization of the nonlinear systems at the state estimates, and the UKF is proposed by virtue of the unscented transformation which can address the deficiency of the linearization method [16, 18]. The PF, based on the sequential importance sampling technique, is particularly useful in dealing with the nonlinear and/or non-Gaussian problem. However, the PF might lead to localization failures due primarily to the sample impoverishment phenomenon, which usually occurs in the case of low process/measurement noises or small number of particles [30]. Also, the high computational complexity in PF significantly hinders its utilization in practical scenarios with the real-time requirement.

It is worth noting that the system noises, including the process noise and measurement noise, are required to be stochastic in the above-mentioned filters [27, 29]. In this case, the mean and covariance, or the probability density of the stochastic noise are utilized to obtain the state estimate [1, 3]. Nevertheless, in the practical application of the wireless localization system, the probabilistic assumptions on the system noises are not always realistic. A more reasonable assumption is that the process and measurement noises are unknown but bounded [25],

⋆ This work was supported in part by the National Natural Science Foundation of China under Grants 61703245, 61933007 and 61873148, the China Postdoctoral Science Foundation under Grant 2018T110702, the Natural Science Foundation of Shandong Province of China under Grant ZR2020MF071, the Royal Society of the UK, and the Alexander von Humboldt Foundation of Germany.

∗ Corresponding author.

Email addresses: `xzbai@163.com` (Xingzhen Bai), `Zidong.Wang@brunel.ac.uk` (Zidong Wang), `zouleicup@gmail.com` (Lei Zou), `zhangzhijingzzj@163.com` (Zhijing Zhang).

which facilitates the development of the so-called set-membership filtering technique. The set-membership filtering does rely on unknown but bounded uncertainties and requires no assumption about the probability distributions of noises [6]. Such a filtering algorithm can provide a set of state estimates in state space which always contains the true states of the system [23]. Up to now, several effective set-membership filtering approaches have been reported in the literature to deal with the target tracking problem, see e.g. [4, 15, 36, 38]. For example, in [21], the set-membership state estimation approach has been successfully applied to estimate the linear position of an octorotor used for radar applications. Ellipsoidal sets that constrain the real system state were calculated, and their sizes were then minimized. In addition, the reliable localization problem has been investigated in [4] for the autonomous mobile robot in an unstructured environment, and the proposed set-valued nonlinear filter has removed the need of an accurate model of the noise statistics and attenuated the influences of linearization errors.

With the revolution of embedded systems and wireless communication technologies, wireless sensing strategies have been widely adopted in various industrial applications with examples including, but are not limited to, the information collecting, signal processing and data transmission. It is often the case in engineering practice that the wireless sensor nodes are subject to the limited energy supply. For the energy-saving purposes, numerous effective energy management methods have been developed in the wireless communication community, and there are two type of representative methods reducing the packet size and the communication rate of sensors [34]. For the latter method, a quite straightforward way is to lower the sampling frequency of sensors, which might result in the loss of useful information, thereby degrading the estimation accuracy. As an alternative solution, the so-called event-triggered mechanism has been developed to adjust the data transmission frequency by considering the characteristic of the measurement change, under which the sensing information is transmitted to the controller/filter only when certain conditions are satisfied [13, 17, 20, 37]. The primary advantage of the event-triggered transmission scheme over the traditional time-triggered one is the improved resource efficiency while guaranteeing the desired control/filtering performance [12, 35]. As such, the event-triggered mechanism has recently attracted increasing research interest in the communication and control communities, see e.g. [14].

It is worth mentioning that the research on event-triggered wireless transmission is of practical importance for wireless localization systems. Nevertheless, a thorough literature search has revealed that the target tracking problem for wireless localization systems with event-triggered transmission has not gained adequate research attention yet, and this motivates us to shorten such a gap. In response to the above discussions, in this paper, we aim to design a set-membership filtering algorithm for the wireless localization systems under the event-triggered transmission scheme, such that the personnel position can be well estimated to further enhance the safety management level in the industrial sites. The main technical contributions of this paper can be summarized as follows: 1) The system model under consideration is subject to the unknown but bounded noises, thereby better reflecting the realistic characteristics of system noises and interferences of the wireless localization system in industrial sites; 2) The component-based event-triggered transmission mechanism is proposed to achieve a trade-off between the filtering performance and the network energy consumption; 3) The particle swarm optimization (PSO) algorithm is adopted to determine the uncertain scaling matrix generated by linearization of the nonlinear measurement function; 4) The developed filter is applied to the personnel tracking in the mine industrial site for improving the safety management capability.

The remainder of this paper is organized as follows. In Section 2, the network structure and dynamic system model are briefly introduced, and the component-based event-triggered mechanism is presented. In Section 3, the set-membership filter under the event-triggered transmission mechanism is designed, and the filtering parameters are obtained through the optimization algorithm with the semi-definite programming. Simulation results are presented in Section 4. Finally, we conclude this paper in Section 5.

2 System Description and Problem Formulation

2.1 Network Structure of Wireless Localization System in Industrial Sites

In the practical application, considering the reliable monitoring requirement, the monitoring region is usually divided into several subregions, and wireless sensor nodes are deployed in different subregions, as shown in Fig. 1. Sensor nodes in the same subregion make up a node cluster, where the related sensors monitor the target of interest cooperatively. In addition, each node cluster has a head node, and the head node is assumed to have higher computing ability and enough power, which connects with the monitoring center by the wired communication. Sensor nodes send their measured data to the corresponding head node, where the estimates are derived via the filtering algorithm and then transmitted to the monitoring center for the further cooperative control implementation.

2.2 System Model

In this section, the target moves in a two-dimensional surveillance region. The target state vector is described

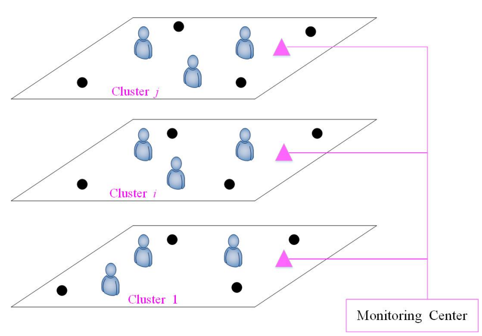

Fig. 1. Network structure of the wireless localization system.

by $x_k = [x_{1,k}\ v_{1,k}\ x_{2,k}\ v_{2,k}]^T$, where $x_{i,k} \in \mathbb{R}$ and $v_{i,k} \in \mathbb{R}$ $(i = 1, 2)$ denote, respectively, the coordinate values of the target positions and velocities along the x_i axis at time t_k. Subsequently, under the consideration of the actual moving characteristics of the target, the system model is given as follows:

$$x_{k+1} = A_k x_k + B_k u_k + \omega_k \tag{1}$$

where

$$A_k = \begin{bmatrix} 1 & \Delta t_k & 0 & 0 \\ 0 & 1 & 0 & 0 \\ 0 & 0 & 1 & \Delta t_k \\ 0 & 0 & 0 & 1 \end{bmatrix}, \quad B_k = \begin{bmatrix} \frac{\Delta t_k^2}{2} & 0 \\ \Delta t_k & 0 \\ 0 & \frac{\Delta t_k^2}{2} \\ 0 & \Delta t_k \end{bmatrix},$$

and $\Delta t_k = t_{k+1} - t_k$ represents the time interval between two successive sampling instants of the wireless localization system. u_k denotes the control input, where $u_k = [u_{1,k}\ u_{2,k}]^T \in \mathbb{R}^2$ with $u_{1,k}$ and $u_{2,k}$ being the accelerations along the x_1 axis and x_2 axis, respectively. In addition, B_k describes the weights of different accelerations. $\omega_k \in \mathbb{R}^4$ stands for the process noise. Moreover, suppose that there are m sensors in one subregion, and the measurement model of the ith sensor node at time t_k is given by

$$y_{i,k} = g_i(x_k) + v_k^i, \tag{2}$$

where $y_{i,k}$ denotes the measurement output, v_k^i is the measurement noise, and $g_i(x_k)$ is the distance function defined as $g_i(x_k) = \sqrt{(x_{1,k} - x_{1,i}^*)^2 + (x_{2,k} - x_{2,i}^*)^2}$, where $x_{1,i}^*$ and $x_{2,i}^*$ denote, respectively, the coordinate values of the ith sensor node along the x_1 and x_2 axes.

For notation simplicity, we denote

$$y_k \triangleq \begin{bmatrix} y_{1,k} \\ \vdots \\ y_{m,k} \end{bmatrix}, \; g(x_k) \triangleq \begin{bmatrix} g_1(x_k) \\ \vdots \\ g_m(x_k) \end{bmatrix}, \; v_k \triangleq \begin{bmatrix} v_k^1 \\ \vdots \\ v_k^m \end{bmatrix}. \tag{3}$$

Then, the measurement output is rewritten as

$$y_k = g(x_k) + v_k. \tag{4}$$

In this paper, the system noises ω_k and v_k are deterministic and satisfy the following assumption.

Assumption 1 *The noise sequences ω_k and v_k are confined to the following ellipsoidal set:*

$$\begin{cases} \mathscr{F}_k \triangleq \{\omega_k : \omega_k^T Q_k^{-1} \omega_k \le 1\} \\ \mathscr{R}_k \triangleq \{\nu_k : v_k^T R_k^{-1} v_k \le 1\} \end{cases} \tag{5}$$

where $Q_k = Q_k^T > 0$ and $R_k = R_k^T > 0$ are known matrices with compatible dimensions characterizing the sizes and orientations of the ellipsoids.

Remark 1 *In this paper, as for the considered target monitoring problem, the wireless sensor nodes are deployed in the monitoring region, and divided into different clusters. It is worth mentioning that there is no connection between sensor nodes of different clusters. When the target enters a subregion, the related sensor nodes in the same cluster would sense the target state cooperatively that facilitates the reliable state estimation for the target. In addition, we consider the distance-based localization algorithm, with which the distance measurements are obtained for tracking the targets to be monitored. In the wireless localization system, the beacon node is fixed on the target, which periodically sends its identity and time stamp information through the wireless radio frequency (RF)channel [32]. After receiving the signals from the target, the sensor nodes can utilize the received signal to evaluate the distance between sensors and the target. The measurement model of the ith sensor node at time t_k is presented as (2), where $y_{i,k}$ denotes the measurement output, and $g_i(x_k)$ represents the distance measurement function given as $g_i(x_k) = \sqrt{(x_{1,k} - x_{1,i}^*)^2 + (x_{2,k} - x_{2,i}^*)^2}$ with $x_{1,i}^*$ and $x_{2,i}^*$ being, respectively, the components of coordinate values of the ith sensor node along the x_1 and x_2 axes.*

Remark 2 *In the practical application, the performance of the wireless localization system is vulnerable to the interferences in the complex environment. In particular, the electromagnetic interference problem is serious in the industrial sites, and the noise sources are generally deterministic, unknown but bounded (by energy or amplitude) [9]. To better reflect the engineering reality of the wireless localization system, in this paper, the process noise ω_k and measurement noise v_k are assumed to be deterministic, unknown but bounded within certain ellipsoidal sets. In this case, most conventional statistic-based filtering schemes (e.g. Kalman filtering) are no longer applicable and thus, the set-membership filtering scheme is put forward to tackle such an issue.*

2.3 Component-Based Event-Triggered Mechanism

With the event-triggered mechanism, sensor nodes determine whether the newly obtained measurement is sent to the filter or not, which is based on the difference between the previously transmitted measurement and the latest measurement. For the wireless localization system, sensor nodes are capable of adjusting the transmission rate according to the dynamic change of sensing signal, which would lower the frequency of the data transmission. In order to improve the energy efficiency of sensor nodes and ensure the desired tracking performance of the localization system, each sensor node examines the triggering condition independently, and the consistency with other nodes in the same cluster is not required. As such, the component-based event-triggered strategy is adopted to decide when the newly obtained measurement is released to the filter for state estimation.

Now, let us elaborate the component-based event-triggered scheme as follows. First, suppose that the event instant sequence of the ith sensor node is denoted as $0 < k_0^i < k_1^i < k_2^i < \cdots < k_t^i < \cdots$, where k_t^i $(t = 0, 1, 2, \ldots)$ represents the $(t+1)$th triggering instant of the ith sensor node. Subsequently, define $\sigma_{i,k} \triangleq y_{i,k_t^i} - y_{i,k}$, which denotes the difference between the latest transmitted value y_{i,k_t^i} and the current value $y_{i,k}$ of the ith sensor node. Furthermore, for the ith sensor node, the event generator function $f_i(\cdot,\cdot)$ is defined as $f_i(\sigma_{i,k}, \delta_i) = \sigma_{i,k}^T \sigma_{i,k} - \delta_i$, where δ_i is a pre-assigned triggering threshold. Under the event-triggered mechanism, the ith sensor node transmits its current measurement data to the filter only when $f_i(\sigma_{i,k}, \delta_i) > 0$ is satisfied. Then, the forthcoming triggering instant is determined iteratively by

$$k_{t+1}^i = \inf\{k \in N | k > k_t^i,\ f_i(\sigma_{i,k}, \delta_i) > 0\}. \tag{6}$$

In addition, the received information of the filter from the ith sensor node can be expressed as

$$\bar{y}_{i,k} = \begin{cases} y_{i,k}, & f_i(\sigma_{i,k}, \delta_i) > 0; \\ y_{i,k_t^i}, & f_i(\sigma_{i,k}, \delta_i) < 0, \end{cases} \tag{7}$$

which implies that

$$\sigma_{i,k} = \begin{cases} 0, & f_i(\sigma_{i,k}, \delta_i) > 0; \\ y_{i,k_t^i} - y_{i,k}, & f_i(\sigma_{i,k}, \delta_i) < 0. \end{cases} \tag{8}$$

Moreover, let $\sigma_k = \begin{bmatrix} \sigma_{1,k}^T & \sigma_{2,k}^T & \dots & \sigma_{m,k}^T \end{bmatrix}^T$, we can get $\sigma_k^T \sigma_k \leq \delta$, where $\delta = \sum_{i=1}^{m} \delta_i$.

Remark 3 *For the purpose of saving energy of wireless network, the component-based event-triggered transmission scheme is employed, with which the measurement transmission of each component (i.e. $y_{i,k}$) is in fact scheduled individually according to its own triggering condition δ_i, which determines the transmission frequency catering for the specific practical requirements. Under the component-based event-triggered mechanism, it focuses on the individual change of each component (or sensor) of the system output, while in the usual event-triggered case, it pays attention to the change of the whole output vector. Considering the characteristics of network architecture of the wireless localization system, the component-based event-triggered mechanism is more suitable for multi-sensor cooperative monitoring system.*

Remark 4 *Under the component-based event-triggered mechanism, the changes of the transmission rate of sensor nodes in the same cluster are independent of each other. In addition, due to the different locations of sensor nodes deployed in the monitoring region, the environmental influences on different sensors may be different, which might cause sensors in the same cluster to change the transmission rate inconsistently. In particular, even under the same triggering threshold δ_i, the triggering number of sensors in the same cluster might be different. Furthermore, the asynchronous transmission of sensors may lead to the consequence that the number of nodes participating in the filtering process at some time instants is less than that of member nodes in the cluster. For instance, the asynchronous transmission of member nodes in the same cluster is illustrated in Fig. 2. In the cluster ι ($\iota \in 1, 2, \cdots, M$), there are 6 member nodes, i.e., $S_{\iota,i}$ ($i = 1, 2, \cdots, 6$), and t_j ($j = 0, 1, \cdots$) is the time instant for the filtering action at the head node. From Fig. 2, we can find that node $S_{\iota,3}$ is not available at time instant t_1, and there are 5 sensors that can transmit information to the filter. Moreover, for the usual event-triggered mechanism (which is implemented based on the whole measurement output), all the sensors would transmit their measurements simultaneously to the filter at each triggering instant. In this regard, the asynchronous transmission phenomenon induced by the component-based event-triggered mechanism will give rise to certain challenges in dealing with the filter design and performance analysis issues.*

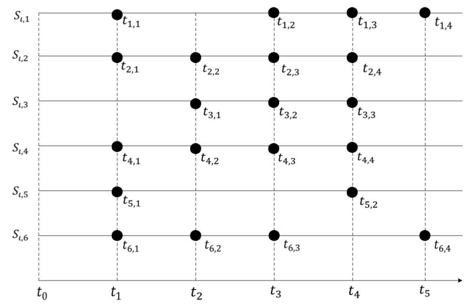

Fig. 2. Asynchronous measurement of sensor nodes in the same cluster.

3 Event-Triggered Set-Membership Filter Design

In this section, we will propose an event-triggered filtering algorithm for the wireless localization system with nonlinear measurement model, and unknown but bounded noises. The sufficient conditions for the existence of the desired filter are developed in terms of the recursive linear matrix inequality (RLMI), such that the true state is guaranteed to reside in a set of state estimates. Moreover, the semi-definite programming method has been proposed to get the optimal estimation set.

3.1 Filter Structure

In this paper, according to (1)-(4) and the proposed event-triggered strategy, the event-triggered filter structure is presented as

$$\hat{x}_{k+1} = A_k \hat{x}_k + B_k u_k + K_k(\bar{y}_k - g(\hat{x}_k)) \tag{9}$$

where $\bar{y}_k = \begin{bmatrix} \bar{y}_{1,k} & \bar{y}_{2,k} & \dots & \bar{y}_{m,k} \end{bmatrix}^T$, $\hat{x}_k$ is the estimate of x_k at time instant k, and K_k is the filter gain to be determined.

From (1) and (9), the one-step ahead filtering error e_{k+1} is written as

$$\begin{aligned} e_{k+1} &= x_{k+1} - \hat{x}_{k+1} \\ &= A_k e_k + \omega_k - K_k(\bar{y}_k - g(\hat{x}_k)). \end{aligned} \tag{10}$$

On the other hand, it follows from the definition of $\sigma_{i,k}$ that the received measurements of the filter from the sensor nodes in the same cluster can be expressed as

$$\bar{y}_k = y_k + \sigma_k. \tag{11}$$

Moreover, the nonlinear measurement function $g(x_k)$ is linearized around the estimate $\hat{x}_k$ as

$$g(x_k) = g(\hat{x}_k) + (G_k + L_k \Delta_k)(x_k - \hat{x}_k) \tag{12}$$

where $G_k = \frac{\partial g(x_k)}{\partial x_k}|_{x_k = \hat{x}_k}$, L_k is a problem-dependent scaling matrix, and Δ_k is an unknown matrix satisfying $\|\Delta_k\| \leq 1$. In this paper, we use the deterministic matrix Δ_k and the scaling matrix L_k to account for the linearization errors induced by the calculation of matrix G_k. For more details, we refer the readers to Appendix C in [4], where a nice interpretation has been presented. If L_k is set to zero, the effects of linearization errors (i.e., the high-order terms in the Taylor expansion) would be simply neglected.

Subsequently, substituting (12) into (4) results in

$$y_k = (G_k + L_k \Delta_k)(x_k - \hat{x}_k) + g(\hat{x}_k) + v_k. \tag{13}$$

Then, combing (10) and (11) with (13), the filtering error is reformulated as

$$
\begin{aligned}
e_{k+1} &= (A_k - K_k(G_k + L_k\Delta_k))(x_k - \hat{x}_k) \\
&\quad - K_k\sigma_k - K_k v_k + \omega_k.
\end{aligned} \tag{14}
$$

3.2 The Optimization of Scaling Matrix

In order to derive the accurate filter parameters, we need to determine the uncertain scaling matrix L_k. From the presentation for the linearization errors in [4], we can get that $L_k = \frac{\sqrt{m}}{2}\|E_k\|\mathrm{diag}\{N_{1,\mathrm{k}}, N_{2,\mathrm{k}}, \ldots, N_{m,\mathrm{k}}\}$, and the positive scalars $N_{i,k}$ satisfy $\|\frac{\partial^2 g_i(x_k)}{\partial x_k^2}\| \leq N_{i,k}$ for all $i = 1, 2, \ldots, m$, where $g_i(x_k)$ is the ith element of $g(x_k)$. Moreover, if $(x_k - \hat{x}_k)^T P_k^{-1}(x_k - \hat{x}_k) \leq 1$, then there exists a vector z_k with $\|z_k\| \leq 1$, which satisfies

$$
x_k = \hat{x}_k + E_k z_k \tag{15}
$$

where E_k is a factorization of $P_k = E_k E_k^T$ [9]. It is clear that the value of $N_{i,k}$ is affected by z_k ($\|z_k\| \leq 1$). Then, we can convert the determination of L_k to the following optimization problem

$$
\begin{aligned}
&N_{i,k} = \max\|\frac{\partial^2 g_i(x_k)}{\partial x_k^2}|_{x_k = \hat{x}_k + E_k z_k}\| \\
&s.t. \qquad \|z_k\| \leq 1.
\end{aligned} \tag{16}
$$

It is well known that PSO is an evolutionary computation algorithm which is easy to implement [11]. Due to its high efficiency, effectiveness in solving difficult optimization problems, and the fast convergence speed to a reasonably good solution, the PSO algorithm has attracted much research attention in a wide range of engineering design problems [33]. In PSO, a population of candidate solutions moves in a d-dimensional search space according to two simple mathematic formulas over the particle's position and velocity.More specifically, each particle's movement is influenced by its local best known position and also the best known positions, which are updated by other particles, in the search space. In this paper, considering the characteristics of PSO and the optimization requirement, we adopt the PSO algorithm to deal with the constrained optimization problem (16). By the iterative approach, the swarm of the particles moves toward the best solutions [19]. The velocity and position of particle l at the next iteration are updated according to the following formulas:

$$
\begin{cases}
v_l(s+1) = \omega v_l(s) + c_1 r_1(p_l(s) - x_l(s)) \\
\qquad\qquad + c_2 r_2(p_g(s) - x_l(s)) \\
x_l(s+1) = x_l(s) + v_l(s+1)
\end{cases} \tag{17}
$$

where $x_l(s) = \begin{bmatrix} x_{l1}(s), \ldots, x_{ld}(s) \end{bmatrix}$ and $v_l(s) = \begin{bmatrix} v_{l1}(s), \ldots, v_{ld}(s) \end{bmatrix}$ are, respectively, the position and velocity of the lth particle at the sth iteration. ω is the inertia weight, c_1 and c_2 are the acceleration coefficients called cognitive and social parameters, respectively. r_1 and r_2 are two random numbers that are distributed uniformly in $[0, 1]$. $p_l(s)$ and $p_g(s)$ are the local best position found by the lth particle and the global best position in the swarm at the sth iteration, respectively. In addition, the speed update formula consists of three parts, as shown in (17). The first term is the inertia velocity of particle, which reflects the memory behavior of particle. It is shown that a larger inertia weight tends to facilitate the global exploration and a smaller inertia weight achieves the local exploration to fine-tune the current search area. The second and the third terms are used to adjust the search direction. The second term tries to tune the search direction toward the best location ever found by the particle itself and the third term is used to change the search direction toward the global best location ever found by all the particles. Because of these two terms, a particle will change its moving direction gradually and coordinately toward those historically found best locations [5, 11]. By the aid of the PSO algorithm, the more accurate value of $N_{i,k}$ is derived through the ergodic search in the search space with the constraint condition $\|z_k\| \leq 1$. As such, we are able to get the appropriate value of parameter L_k.

3.3 Main Results

Firstly, let us recall the following two lemmas, which will be used in the subsequent developments.

Lemma 1 *(*S-Procedure *[2]) Let $\psi_0(\cdot), \psi_1(\cdot), \ldots, \psi_p(\cdot)$ be quadratic functions of the variable $\varsigma \in \mathbb{R}^n$, $\psi_i(\varsigma) \triangleq \varsigma^T X_i \varsigma (i = 0, 1, \ldots, p)$: where $X_i = X_i^T$. If there exist $\tau_1 \geq 0, \ldots, \tau_p \geq 0$ such that $X_0 - \sum_{i=1}^p \tau_i X_i \leq 0$, then the following is true*

$$
\psi_1(\varsigma) \leq 0, \ldots, \psi_p(\varsigma) \leq 0 \rightarrow \psi_0(\varsigma) \leq 0. \tag{18}
$$

Lemma 2 *(*Schur Complement Equivalence*) Given constant matrices $\mathcal{S}_1$, $\mathcal{S}_2$, and $\mathcal{S}_3$ where $\mathcal{S}_1 = \mathcal{S}_1^T$ and $\mathcal{S}_2 = \mathcal{S}_2^T > 0$, then $\mathcal{S}_1 + \mathcal{S}_3^T \mathcal{S}_2^{-1} \mathcal{S}_3 \leq 0$ if and only if*

$$
\begin{bmatrix} \mathcal{S}_1 & \mathcal{S}_3^T \\ \mathcal{S}_3 & -\mathcal{S}_2 \end{bmatrix} < 0 \quad \text{or} \quad \begin{bmatrix} -\mathcal{S}_2 & \mathcal{S}_3 \\ \mathcal{S}_3^T & \mathcal{S}_1 \end{bmatrix} < 0. \tag{19}
$$

Before proceeding further, we give the following assumption.

Assumption 2 *The initial state x_0 and its estimate $\hat{x}_0$ satisfy*

$$
(x_0 - \hat{x}_0)^T P_0^{-1}(x_0 - \hat{x}_0) \leq 1 \tag{20}
$$

where $P_0 = P_0^T > 0$ is a given positive definite matrix.

The objective of this paper is to determine an ellipsoid

$$
\begin{aligned}
\mathscr{X}_{k+1} \triangleq \{x_{k+1} :\ &(x_{k+1} - \hat{x}_{k+1})^T P_{k+1}^{-1} \\
&\times (x_{k+1} - \hat{x}_{k+1}) \leq 1\}
\end{aligned} \tag{21}
$$

for the state x_{k+1}, given the measurement information $\bar{y}_k$ at time instant k for the process noise $\omega_k \in \mathscr{F}_k$ and the measurement noise $\nu_k \in \mathscr{R}_k$.

The following theorem presents a sufficient condition for the solvability of the formulated event-triggered set-membership filtering problem.

Theorem 1 *For the wireless localization system in the form of (1) and (4), and the component-based event-triggered transmission mechanism with $\sigma_k^T \sigma_k \leq \delta$, suppose that the state x_k belongs to its state estimation ellipsoid $(x_k - \hat{x}_k)^T P_k^{-1}(x_k - \hat{x}_k) \leq 1$. Then, the one-step ahead state x_{k+1} resides in its state estimation ellipsoid $(x_{k+1} - \hat{x}_{k+1})^T P_{k+1}^{-1}(x_{k+1} - \hat{x}_{k+1}) \leq 1$, if there exist $P_{k+1} > 0$, K_k, $\lambda_{1,k} > 0$, $\lambda_{2,k} > 0$, $\lambda_{3,k} > 0$, $\lambda_{4,k} > 0$ and $\lambda_{5,k} > 0$, such that*

$$
\begin{bmatrix} \Omega_k & \Pi_k^T \\ \Pi_k & -P_{k+1} \end{bmatrix} < 0 \tag{22}
$$

where

$$\Omega_k = \mathrm{diag}\Big\{\lambda_{1,\mathrm{k}} + \lambda_{2,\mathrm{k}} + \lambda_{5,\mathrm{k}} + \lambda_{4,\mathrm{k}}\delta - 1, \lambda_{3,\mathrm{k}}\mathrm{E}_{\mathrm{k}}^{\mathrm{T}}\mathrm{E}_{\mathrm{k}} - \lambda_{1,k}\mathrm{I}, -\lambda_{2,k}Q_k^{-1}, -\lambda_{3,k}I, -\lambda_{4,k}I, -\lambda_{5,k}R_k^{-1}\Big\}$$

$$\Pi_k = \Big[0 \;\; (A_k - K_kG_k)E_k \;\; 1 \;\; -K_kL_k \;\; -K_k \;\; -K_k\Big].$$

In addition, the center of the state estimate ellipsoid is determined by (9).

Proof: In view of the condition $(x_k - \hat{x}_k)^T P_k^{-1}(x_k - \hat{x}_k) \leq 1$, it follows from (14) and (15) that

$$\begin{aligned} e_{k+1} &= x_{k+1} - \hat{x}_{k+1} \\ &= A_kE_kz_k + \omega_k - K_k(G_k + L_k\Delta_k)E_kz \\ &\quad - K_k\sigma_k - K_kv_k. \end{aligned} \tag{23}$$

Denoting $\aleph_k = \Delta_k E_k z_k$ with $\|\Delta_k\| \leq 1$. we have

$$\aleph_k^T\aleph_k \leq z_k^T E_k^T E_k z_k. \tag{24}$$

Then, the filtering error is expressed by

$$\begin{aligned} e_{k+1} &= (A_k - K_kG_k)E_kz_k + \omega_k \\ &\quad - K_kL_k\aleph_k - K_k\sigma_k - K_kv_k. \end{aligned} \tag{25}$$

Next, letting

$$\eta_k \triangleq \Big[1 \;\; z_k^T \;\; \omega_k^T \;\; \aleph_k^T \;\; \sigma_k^T \;\; v_k^T\Big]^T, \tag{26}$$

the filtering error is further rewritten in the compact form with $e_{k+1} = \Pi_k\eta_k$, where

$$\Pi_k = \Big[0 \;\; (A_k - K_kG_k)E_k \;\; 1 \;\; -K_kL_k \;\; -K_k \;\; -K_k\Big]. \tag{27}$$

Therefore, the one-step ahead filtering error constraint $(x_{k+1} - \hat{x}_{k+1})^T P_{k+1}^{-1}(x_{k+1} - \hat{x}_{k+1}) \leq 1$ can be reformulated as

$$\eta_k^T\Big[\Pi_k^T P_{k+1}^{-1}\Pi_k - \mathrm{diag}\{1,0,0,0,0,0\}\Big]\eta_{\mathrm{k}} \leq 0. \tag{28}$$

It follows from (5), (9) and (24) that the unknown variables z_k, ω_k, v_k, σ_k and $\aleph_k$ satisfy:

$$\begin{cases} \|z_k\| \leq 1, \quad \sigma_k^T\sigma_k \leq \delta, \quad \aleph_k^T\aleph_k \leq z_k^TE_k^TE_kz_k, \\ \omega_k^TQ_k^{-1}\omega_k \leq 1, \quad v_k^TR_k^{-1}v_k \leq 1 \end{cases} \tag{29}$$

which are rewritten by means of η_k in (26) as follows:

$$\begin{cases} \eta_k^T\mathrm{diag}\{-1, I, 0, 0, 0, 0\}\eta_k \leq 0 \\ \eta_k^T\mathrm{diag}\{-1, 0, Q_k^{-1}, 0, 0, 0\}\eta_k \leq 0 \\ \eta_k^T\mathrm{diag}\{0, -E_k^{\mathrm{T}}E_k, 0, I, 0, 0\}\eta_k \leq 0 \\ \eta_k^T\mathrm{diag}\{-\delta, 0, 0, 0, I, 0\}\eta_k \leq 0 \\ \eta_k^T\mathrm{diag}\{-1, 0, 0, 0, 0, R_k^{-1}\}\eta_k \leq 0. \end{cases} \tag{30}$$

By resorting to the S-procedure in Lemma 1, the inequality (28) holds if there exist positive scalars $\lambda_{1,k}$, $\lambda_{2,k}$, $\lambda_{3,k}$, $\lambda_{4,k}$ and $\lambda_{5,k}$ such that the following inequality is true:

$$\begin{aligned} &\Pi_k^TP_{k+1}^{-1}\Pi_k - \mathrm{diag}\{1,0,0,0,0,0\} \\ &- \lambda_{1,k}\mathrm{diag}\{-1, I, 0, 0, 0, 0\} \\ &- \lambda_{2,k}\mathrm{diag}\{-1, 0, Q_k^{-1}, 0, 0, 0\} \\ &- \lambda_{3,k}\mathrm{diag}\{0, -E_k^{\mathrm{T}}E_k, 0, \mathrm{I}, 0, 0\} \\ &- \lambda_{4,k}\mathrm{diag}\{-\delta, 0, 0, 0, I, 0\} \\ &- \lambda_{5,k}\mathrm{diag}\{-1, 0, 0, 0, 0, R_k^{-1}\} \leq 0. \end{aligned} \tag{31}$$

Furthermore, denote

$$\Omega_k = \mathrm{diag}\Big\{\lambda_{1,\mathrm{k}} + \lambda_{2,\mathrm{k}} + \lambda_{5,\mathrm{k}} + \lambda_{4,\mathrm{k}}\delta - 1, \lambda_{3,\mathrm{k}}E_k^{\mathrm{T}}E_k - \lambda_1 I, -\lambda_{2,k}Q_k^{-1}, -\lambda_{3,k}I, -\lambda_{4,k}I, -\lambda_{5,k}R_k^{-1}\Big\}. \tag{32}$$

It is clear that (31) can be rewritten as

$$\Pi_k^TP_{k+1}^{-1}\Pi_k + \Omega_k \leq 0. \tag{33}$$

By applying Lemma 2, it is not difficult to verify that (33) is equivalent to

$$\begin{bmatrix} \Omega_k & \Pi_k^T \\ \Pi_k & -P_{k+1} \end{bmatrix} < 0. \tag{34}$$

Hence, if there exist the filter parameters K_k, and scalars $\lambda_{1,k} > 0$, $\lambda_{2,k} > 0$, $\lambda_{3,k} > 0$, $\lambda_{4,k} > 0$, $\lambda_{5,k} > 0$ such that (22) holds, the one-step ahead state x_{k+1} resides in its state estimation ellipsoid $(x_{k+1} - \hat{x}_{k+1})^T P_{k+1}^{-1}(x_{k+1} - \hat{x}_{k+1}) \leq 1$. The proof is now complete.

Theorem 1 has outlined the principle of determining the filtering parameters by solving the RLMI. However, it should be pointed out that the proposed method has not provided an optimal solution (i.e., a minimal state estimation ellipsoid). As such, we now proceed to tackle the optimization problem by minimizing the trace of P_{k+1} at each time instant. In this paper, the convex optimization approach [31] is utilized to determine the optimal state estimation ellipsoid. To be more specific, P_{k+1} is obtained by solving the following optimization problem:

$$\min_{P_{k+1}, K_k, \lambda_{1,k}\geq 0, \lambda_{2,k}\geq 0, \lambda_{3,k}\geq 0, \lambda_{4,k}\geq 0, \lambda_{5,k}\geq 0} \mathrm{trace}(P_{\mathrm{k+1}}) \tag{35}$$

subject to (22), where $\mathrm{trace}(P_{\mathrm{k+1}})$ denotes the trace of P_{k+1}.

Subsequently, an iterative algorithm can be obtained to compute the sequences of the filtering parameters $\{K_k\}_{k>0}$.

Algorithm 1: Event-triggered set-membership filtering for target tracking

---

Step 1. Initialization: Set $k = 0$ and the maximum computation step $k_{\max}$, set the positive definite matrices Q_k and R_k to satisfy (5), select the initial values of x_0 and $\hat{x}_0$ satisfying (20), and set the triggering threshold δ_i for all $i = 1, 2, \ldots, m$.

Step 2. With the obtained $\hat{x}_k$ and P_k, use the PSO algorithm to get $N_{i,k}$ $(i = 1, 2, \ldots, m)$, thereby obtaining L_k.

Step 3. With the obtained $\hat{x}_k$, P_k and L_k, solve the convex optimization problem (35) to obtain K_k, P_{k+1} and $\lambda_{j,k}(i = j, \ldots, 5)$.

Step 4. With the obtained $\hat{x}_k$ and K_k, compute $\hat{x}_{k+1}$ according to (9)

Step 5. Set $k = k + 1$, if $k > k_{max}$, exit. Otherwise, go to step 2.

Remark 5 *In this paper, with the component-based event-triggered mechanism, the number of valid sensors nodes accessing to the filtering process is time-varying. In order to deal with this challenging issue, we have used the zero-order holder to guarantee that the received measurement signal of the filter is vector with fixed dimension (which equals to the dimension of y_k). More specifically, under the event-triggered mechanism, sensor node i*

would transmit it current measurement to the filter only when $f_i(\sigma_{i,k}, \delta_i) > 0$. Otherwise, when $f_i(\sigma_{i,k}, \delta_i) < 0$, the filter cannot receive information from sensor node i, and the latest transmitted one y_{i,k_t^i} would be used to the filtering process instead of $y_{i,k}$. As such, if all sensor nodes in the same cluster do not transmit data to the filter at the same time, the filter would use their latest transmission values of sensor nodes to estimate the target state of this time. Then, the difficulty brought by the "time-varying valid node" is converted to dealing with the effects of σ_k on the subsequent filter design and analyses. In this paper, to tackle the effects of σ_k, we employ the prescribed triggering condition which can be rewritten as a quadratic constraint (see the second formula of eq. (29)). Subsequently, by using S-procedure, this quadratic constraint can be easily dealt with and reflected in the obtained RLMIs. In addition, we have designed the filter by using the constraint $\sigma_k^T \sigma_k \leq \delta$ (which is in fact the compact form of the original event-triggered condition $f_i(\sigma_{i,k}, \delta_i) > 0$), since the employment of $\sigma_k^T \sigma_k \leq \delta$ will make our result (Theorem 1) more concise yet efficient, though some conservatism exists.

Remark 6 *In Theorem 1, with the condition (22) satisfied, there exists an estimation ellipsoidal set $\{x_{k+1} | (x_{k+1} - \hat{x}_{k+1})^T P_{k+1}^{-1} (x_{k+1} - \hat{x}_{k+1}) \leq 1\}$, and the one-step ahead state x_{k+1} will reside in this ellipsoidal set. There are mainly three factors affecting the bounds of the system state, which are given as follows: 1) the system dynamics reflected in A_k, G_k, L_k; 2) the matrix P_0, which reflects the bounds of the initial estimation error, and the larger P_0^{-1} is, the larger the upper bound is; and 3) Q_k and R_k that characterize the bounds of the external process noise and measurement noise, respectively, and Q_k^{-1} and R_k^{-1} are with the same law with P_0^{-1}. Moreover, as an essential parameter in (22), the scalar δ is capable of indicating the triggering frequency. A low value of δ would give rise to a high triggering frequency and enlarge the feasible region of the LMI condition. Similarly, the matrices Q_k and R_k would reflect the bounds of the process noise and the measurement noise, respectively. The low values of Q_k and R_k would help to enlarge the feasible region of (22), which might lead to a small value of P_{k+1}.*

Remark 7 *In this paper, we have adopted the method of minimizing the trace of P_{k+1}. In fact, the volume is an effective measure for the size of ellipsoids [8], and the filter parameters can be determined by optimizing the volume of the obtained ellipsoidal sets. However, it should be noted that calculating the volume of the ellipsoidal set $\{e_{k+1} |\ e_{k+1}^T P_{k+1}^{-1} e_{k+1} \leq 1\}$ is more difficult than the trace of the matrix P_{k+1}, that would inevitably lead to more complexities in the design of filter and the realization of the filtering algorithm. Furthermore, the trace of the matrix P_{k+1} is capable of reflecting the volume of the obtained ellipsoid. The adopted approach in this paper owns the following merits: 1) the trace of P_{k+1} is the sum of the semi-axes of the ellipsoid $\{e_{k+1} | e_{k+1}^T P_{k+1} e_{k+1} = 1\}$, by which the size of the ellipsoidal set $\{e_{k+1} | e_{k+1}^T P_{k+1} e_{k+1} \leq 1\}$ can be reflected effectively; and 2) minimizing the trace of P_{k+1} subject to (22) is a convex optimization problem that is easy to solve by using MATLAB LMI Toolbox.*

Remark 8 *It should be mentioned that if the nonlinearity in the measurement model given by (4) is dealt with using the traditional EKF, the high-order terms in the Taylor expansion would be simply neglected, which inevitably leads to conservatism in certain cases. In this paper, similar to [4], the scaling matrix L_k and deterministic matrix Δ_k have been utilized, as shown in (12), to account for the linearization errors resulting from the calculation of matrix G_k, where L_k is related to $N_{i,k}$ that satisfies $\| \frac{\partial^2 g_i(x_k)}{\partial x_k^2} \| \leq N_{i,k}$ $(i = 1, 2, \cdots, m)$. For the optimization problem shown in (16), we can easily find from the analytic expression of $g_i(x_k)$ that $g_i(x_k)$ is twice times continuously differentiable, and the maximum problem $\arg\max_{\|z_k \leq 1\|} \| \frac{\partial^2 g_i(x_k)}{\partial x_k^2} |_{x_k = \hat{x}_k + E_k z_k} \|$ is feasible. In this paper, considering the characteristics of the PSO algorithm and the optimization requirement, the PSO algorithm has been adopted to derive the optimal solutions of $N_{i,k}$ through the ergodic search in the search space with the constraint condition $\|z_k\| \leq 1$. As such, we are able to get the appropriate value of parameter L_k. In order to get a minimal state estimation ellipsoid containing the true state of the target, an optimization problem has been formulated in (35) to obtain the optimal parameters, which can be solved by the existing semi-definite programming methods [22].*

4 Wireless Localization over Wireless Sensor Networks in Industrial Sites

In this section, we present an application example for the wireless localization system to demonstrate the superiority of the proposed filtering algorithm. For the purpose of improving the mine personnel-safety monitoring capability, wireless sensors are deployed in the multilayer maintenance platforms above the mine wellhead to monitor the workers staying in this region. As shown in Fig. 3, on one of the platforms, six sensors form a node cluster. The sensor nodes in the same cluster sense the signals from the target of interest and further transmit them to the filter. Then, the position estimate of the target is obtained via the proposed filtering algorithm and transmitted to the monitor center for the cooperative control of the mine hoister.

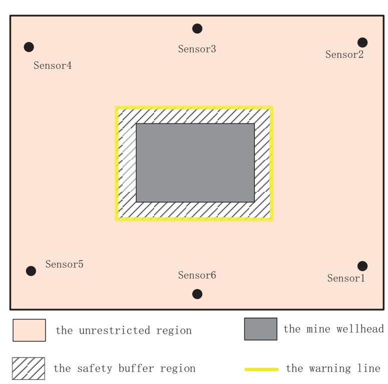

Fig. 3. Maintenance platform of mine hoister.

In this simulation, as shown in Fig. 3, six wireless sensors are deployed to perform the monitoring task cooperatively, and the positions of Sensors 1-6 are $(20, 2)$, $(20, 12)$, $(10, 14)$, $(0, 12)$, $(0, 2)$ and $(10, 0)$, respectively. The target moves along certain elliptical trajectory with a constant speed. The sampling period is $\Delta t_k = 200$ ms and the initial position of the target is $(10, 1)$. The initial conditions of the filter are chosen as $\hat{x}_0 = [10\ \ 0.13\ \ 1\ \ 0]^T$ and $P_0 = I$. Set $Q = 0.01I$ and $R = 0.01I$. In addition, the parameters related to the PSO algorithm are set as follows: the particle number $N_p = 20$, the maximum generation number is 100, $\omega = 1$ and $c_1 = c_2 = 1.5$. Furthermore, in order to show the advantage of the proposed filtering algorithm, the mean square error (MSE) is adopted to verify the filtering accuracy of the target location. Let $E_{c,i} = (1/N_s)\sum_{k=1}^{N_s}(x_{i,k} - \hat{x}_{i,k})^2$ be the MSE of $x_{i,k}$ $(i = 1, 2)$, and $E_p = (1/N_s)\sum_{k=1}^{N_s}[(x_{1,k} - \hat{x}_{1,k})^2 + (x_{2,k} - \hat{x}_{2,k})^2]$ be the MSE of the target position estimate, where $N_s = 100$ is the number of simulations, $N_t = 200$ is the number of sampling instants, and $\hat{x}_{i,k}$ is the estimate of $x_{i,k}$.

From Algorithm 1 developed in Section 3, the filter parameters can be derived recursively and the simulation results are shown in Figs. 4-7. In particular, in order to reveal the superior performance of the proposed filter, we first conduct the experiment with the event-triggering threshold $\delta = 0.6$. During the target tracking process, as depicted in Fig. 4(a), six sensors trigger the data transmission independently. Fig. 4(b) plots the average triggering times of these six sensors in the same cluster, from which we can observe that the triggering times of different sensors maybe different. Specifically, the average number of triggering times of Sensor 3 is 35, and that of Sensor 4 is 42. Moreover, Fig. 5 plots the actual moving trajectory and the estimated trajectory of the target in the two-dimensional plane, and Fig. 6(a) and (b) display, respectively, the actual coordinates $x_{1,k}$ and $x_{2,k}$ and their corresponding estimates. The MSE of the target position estimate is about $E_p = 0.31$, and the M-SEs of $x_{1,k}$ and $x_{2,k}$ coordinates are about $E_{c,1} = 0.16$ and $E_{c,2} = 0.15$, respectively. In addition, Fig. 7(a) and (b) show that the estimates of $x_{1,k}$ and $x_{2,k}$ both reside between their upper bounds and lower bounds, which implies that the estimated ellipsoids always contain the true states.

In the data transmission process of wireless networks, the energy consumption is mainly related to the amount of transmitted data and the transmission distance [10].

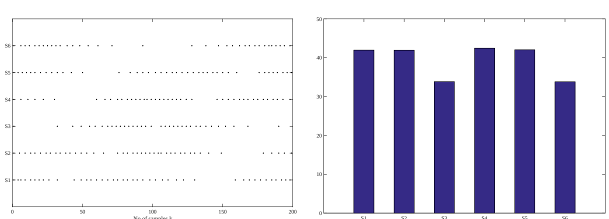

(a) (b)

Fig. 4. Triggering sequences and average triggering times of sensors with $\delta = 0.6$. (a)Triggering sequences for $\delta = 0.6$. (b)Average triggering times of sensors with $\delta = 0.6$.

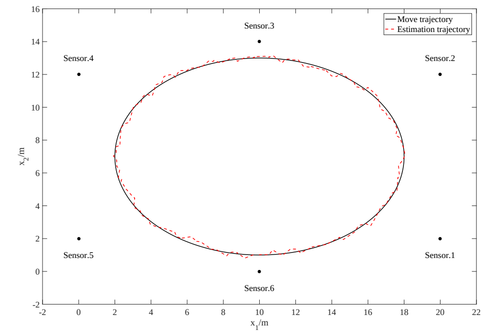

Fig. 5. Actual and estimated trajectories of the target.

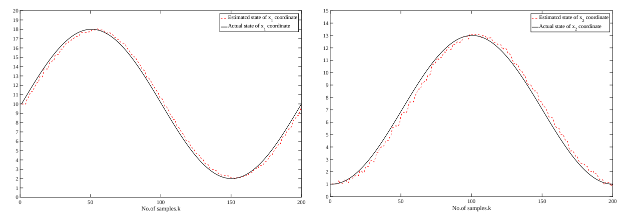

(a) (b)

Fig. 6. True state and its estimation. (a)The true $x_{1,k}$ coordinate and its estimation. (b)The true $x_{2,k}$ coordinate and its estimation.

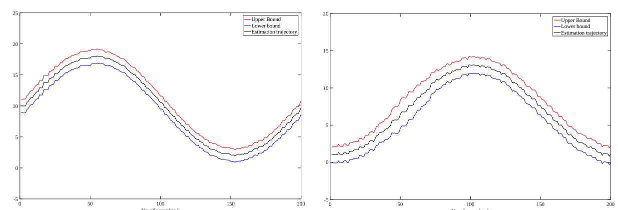

(a) (b)

Fig. 7. The state estimation and its upper and lower bounds. (a) The estimation of $x_{1,k}$ and its upper and lower bounds. (b) The estimation of $x_{2,k}$ and its upper and lower bounds.

For the wireless localization system considered in this paper, the transmission distance under consideration is fixed. Accordingly, the energy consumption is dependent on the data transmission rate, which is determined by the triggering frequencies of sensor nodes. In order to reveal the impact from the proposed event-triggered mechanism on the filtering performance, we conduct simulations with different triggering thresholds. Tab. 1 shows the MSEs of the proposed filtering algorithm at ten time instants with $\delta = 0, 0.2, 0.4, 0.6, 0.8, 1.0$. Note that $\delta = 0$ means sensor nodes transmit their measurements with no triggering constraint. It can be observed obviously that the filtering performance is improved as the threshold decreases. In addition, Tab. 2 presents the triggering times of different sensor nodes in the same cluster with different thresholds, where S and N denote the sensor number and the triggering times of sensor nodes, respectively. It can be seen that the triggering times of sensor nodes will decrease as the thresholds increase. For instance, the average number of transmission of Sensor 2 is about 59 when $\delta = 0.4$, and that is about 42 when $\delta = 0.6$. Obviously, the energy consumption of sensor nodes would be reduced by increasing the thresholds δ.

From Tab. 1 and Tab. 2, it is clear that decreasing the transmission frequency by increasing δ can significantly reduce the energy consumption of sensor nodes at the expense of sacrificing certain filtering performance. Therefore, an appropriate threshold should be selected in practice to achieve a trade-off between the energy conservation of wireless sensor nodes and the filtering performance of the wireless localization system.

Table 1
The MSE of different sampling instants under different triggering thresholds.

E_p N_t δ	20	40	60	80	100	120	140	160	180	200
0	0.02	0.01	0.01	0.02	0.03	0.02	0.01	0.01	0.02	0.02
0.2	0.08	0.08	0.08	0.09	0.10	0.10	0.07	0.06	0.08	0.07
0.4	0.19	0.20	0.21	0.18	0.18	0.18	0.17	0.20	0.19	0.19
0.6	0.37	0.32	0.28	0.34	0.32	0.28	0.29	0.31	0.30	0.29
0.8	0.58	0.52	0.61	0.64	0.56	0.50	0.62	0.59	0.64	0.59
1.0	0.88	1.04	0.96	1.06	0.85	0.83	0.96	0.64	1.02	0.86

Table 2
Triggering times of sensors with different triggering thresholds.

N S δ	$S1$	$S2$	$S3$	$S4$	$S5$	$S6$
0.2	98	99	79	98	98	79
0.4	59	59	48	59	59	48
0.6	42	42	35	42	42	34
0.8	33	33	27	32	32	27
1.0	26	27	22	25	26	22

5 Conclusion

In this paper, we have focused on the moving target tracking problem for the wireless localization system with hope to improve the personnel safety monitor capability in industrial sites. Considering the fact that the wireless information transmission is vulnerable to the unknown but bounded noise in complex industrial environment, the ellipsoidal state estimation approach has been adopted to provide a set of state estimates in state space that contains the true state of the system. Moreover, the component-based event-triggered mechanism has been proposed to adjust the signal transmission frequency to reduce the unnecessary information transmission, thereby saving the communication cost. A sufficient condition for the existence of filter parameters has been established. In addition, the semi-definite programming method has been employed to get the optimal estimation set. Subsequently, an event-triggered set-membership filtering algorithm has been developed for computing the state estimate ellipsoid to enhance the reliability of the wireless localization system. Finally, the personnel tracking problem in a mine equipment maintenance platform has been considered to illustrate the effectiveness of the proposed filtering algorithm. Further research topics include the moving target tracking problem for the wireless localization system subject to various communication protocols [28, 39].

References

[1] Basin, M. V., Ramirez, P. C. R., & Guerra-Avellaneda, F. (2018). Continuous fixed-time controller design for mechatronic systems with incomplete measurements. *IEEE-ASME Transactions on Mechatronics*, 23(1), 57-67.

[2] Boyd, S., El Ghaoui, L., Feron, E., & Balakrishnan, V. (1994). *Linear matrix inequalities in system and control theory*, Philadelphia, PA: SIAM.

[3] Caballero-Águila, R., Hermoso-Carazo A., & Linares-Pérez, J. (2019). Networked distributed fusion estimation under uncertain outputs with random transmission delays, packet losses and multi-packet processing. *Signal Processing*, 156, 71-83.

[4] Calafiore, G. (2005). Reliable localization using set-valued nonlinear filters. *IEEE Transactions on Systems, Man, and Cybernetics-Part A: System and Humans*, 35(2), 189-197.

[5] Chen, T. Y., & Chi, T. M.. (2010). On the improvements of the particle swarm optimization algorithm. *Advances in Engineering Software*, 41(2), 229-239.

[6] Combastel, C. (2015). Zonotopes and Kalman observers: Gain optimality under distinct uncertainty paradigms and robust convergence. *Automatica*, 55, 265-273.

[7] Derr, K., & Manic, M. (2015). Wireless sensor networks-node localization for various industry problems. *IEEE Transactions on Industrial Informatics*, 11(3), 752-762.

[8] Durieu, C., Walter, É., & Polyak, B. (2001). Multi-input multi-output ellipsoidal state bounding. *Journal of Optimization Theory and Applications*, 111(2), 273-303.

[9] El Ghaoui, L., & Calafiore, G. (2001). Robust filtering for discrete-time systems with bounded noise and parametric uncertainty. *IEEE Transactions on Automatic Control*, 46(7), 1084-1089.

[10] Heinzelman, W. B., Chandrakasan, A. P., & Balakrishnan, H. (2002). An application-specific protocol architecture for wireless microsensor networks. *IEEE Transactions on Wireless Communications*, 1(4), 660-670.

[11] Ho, S. L., Yang, S. Y., Ni, G. Z., & Wong, K. F. (2007). An improved pso method with application to multimodal functions of inverse problems. *IEEE Transactions on Magnetics*, 43(4), 1597-1600.

[12] Hu, J., Wang, Z., Liu, G.-P., Jia, C. & Williams, J. (2020). Event-triggered recursive state estimation for dynamical networks under randomly switching topologies and multiple missing measurements. *Automatica*, 115, art. no. 108908.

[13] Hu, S., Yue, D., Han, Q.-L., Xie, X., Chen, X. & Dou, C. (2019). Observer-based event-triggered control for networked linear systems subject to denial-of-service attacks. *IEEE Transactions on Magnetics*, 50(5), 1952-1964.

[14] Li, Q., Shen, B., Wang, Z., & Sheng, W. (2020). Recursive distributed filtering over sensor networks on Gilbert-Elliott channels: A dynamic event-triggered approach. *Automatica*, 113, art. no. 108681.

[15] Li, X., Han, F., Hou, N., Dong H., & Liu. H. (2020). Set-membership filtering for piecewise linear systems with censored measurements under Round-Robin protocol. *International Journal of Systems Science*, 51(9), 1578-1588.

[16] Liu, D., Wang, Z., Liu, Y., & Alsaadi, F. E.(2020). Extended Kalman filtering subject to random transmission delays: Dealing with packet disorders. *Information Fusion*, 60, 80-86.

[17] Liu, J., Yang, M., Tian, E., Cao, J., & Fei, S.(2019). Event-based security controller design for state-dependent uncertain systems under hybrid-attacks and its application to electronic circuits. *IEEE Transactions on Circuits and Systems I: Regular Papers*, 66(12), 4817-4828.

[18] Liu, S., Wang, Z., Chen, Y., & Wei, G.(2020). Protocol-based unscented Kalman filtering in the presence of stochastic uncertainties. *IEEE Transactions on Automatic Control*, 65(3), 1303-1309.

[19] Liu, W., Wang, Z., Yuan, Y., Zeng, N., Hone, K., & Liu, X.(2021). A novel sigmoid-function-based adaptive weighted particle swarm optimizer. *IEEE Transactions on Cybernetics*, 51(2), 1085-1093.

[20] Liu, Y., Wang, Z., Yuan, Y., & Liu, W.(2019). Event-triggered partial-nodes-based state estimation for delayed complex networks with bounded distributed delays. *IEEE Transactions on Systems, Man, and Cybernetics: Systems*, 49(6), 1088-1098.

[21] Merhy, D., Stoica Maniu, C., Alamo, T., Camacho, E. F., Ben Chabane, S., & Chevet, T., et al. (2020). Guaranteed set-membership state estimation of an octorotor's position for radar applications. *International Journal of Control*, 93(11), 2760-2770.

[22] Nesterov, Y., & Nemirovski, A.(1994). *Interior Point Polynomial Methods in Convex Programming: Theory and Applications*. Philadelphia, PA, USA: SIAM.

[23] Orihuela, L., Roshany-Yamchi, S., García, R. A., & Millán, Pablo. (2017). Distributed set-membership observers for interconnected multi-rate systems. *Automatica*, 85, 221-226.

[24] Pak, J. M., Ahn, C. K., Shmaliy, Y. S., Shi, P., & Lim, M. T. (2017). Accurate and reliable human localization using composite Particle/FIR filtering. *IEEE Transactions on Human-Machine Systems*, 47(3), 332-342.

[25] Polyak, B. T., Nazin, S. A., Durieu, C., & Walter, E. (2004). Ellipsoidal parameter or state estimation under model uncertainty. *Automatica*, 40, 1171-1179.

[26] Seifzadeh, S., Khaleghi, B., & Karray, F. (2015). Distributed soft-data constrained multi-model particle filter. *IEEE Transactions on Cybernetics*, 45(3), 384-394.

[27] Shen, B., Wang, Z., Wang, D., & Li, Q.(2020). State-saturated recursive filter design for stochastic time-varying nonlinear complex networks under deception attacks. *IEEE Transactions on Neural Networks and Learning Systems*, 31(10), 3788-3800.

[28] Shen, Y., Wang, Z., Shen, B., & Alsaadi, F. E.(2020). Fusion estimation for multi-rate linear repetitive processes under weighted Try-Once-Discard protocol. *Information Fusion*, 55, 281-291.

[29] Tan, H., Shen, B., Peng, K. & Liu, H. (2020). Robust recursive filtering for uncertain stochastic systems with amplify-and-forward relays, *International Journal of Systems Science*, 51(7), 1188-1199.

[30] Thrun, S., Burgard, W., & Fox, D. (2005). *Probabilistic Robotics*, Cambridge, MA, USA: MIT Press.

[31] Vandenberghet, L., & Boyd, S.(1996). Semidefinite programming. *SIAM Review*, 38(1), 49-95.

[32] Wang, X., Fu, M., & Zhang, H. (2012). Target tracking in wireless sensor networks based on the combination of KF and MLE using distance measurements. *IEEE Transactions on Mobile Computing*, 11(4), 2760-2770.

[33] Zeng, N., Wang, Z., Li, Y., Du, M., & Liu, X. (2012). A hybrid EKF and switching PSO algorithm for joint state and parameter estimation of lateral flow immunoassay models. *IEEE/ACM transactions on computational biology and bioinformatics*, 9(2), 321-329.

[34] Zhang, D., Yu, L., & Zhang, W.-A. (2015). Energy efficient distributed filtering for a class of nonlinear systems in sensor networks. *IEEE Sensors Journal*, 15(5), 3026-3036.

[35] Zhao, D., Wang, Z., Wei, G., & Han, Q.-L. (2020). A dynamic event-triggered approach to observer-based PID security control subject to deception attacks. *Automatica*, 120, art. no. 109128.

[36] Zhao, Z., Wang, Z., Zou, L., & Guo, J. (2020). Set-membership filtering for time-varying complex networks with uniform quantisations over randomly delayed redundant channels. *International Journal of Systems Science*, 51(16), 3364-3377.

[37] Zou, L., Wang Z., & Zhou, D. H. (2020). Moving horizon estimation with non-uniform sampling under component-based dynamic event-triggered transmission. *Automatica*, 120, art. no. 109154.

[38] Zou, L., Wang Z., Geng, H., & Liu, X. (2021). Set-membership filtering subject to impulsive measurement outliers: A recursive algorithm. *IEEE/CAA Journal of Automatica Sinica*, 8(2), 377-388.

[39] Zou, L., Wang Z., Hu, J., Liu, Y., & Liu, X. (2021). Communication-protocol-based analysis and synthesis of networked systems: Progress, prospects and challenges. *International Journal of Systems Science*, in press, DOI: 10.1080/00207721.2021.1917721.